

Research Paper

# Prospective Study of $^{68}\text{Ga}$ -NOTA-NFB: Radiation Dosimetry in Healthy Volunteers and First Application in Glioma Patients

Zhe Wang<sup>1\*</sup>, Mingru Zhang<sup>1\*</sup>, Liang Wang<sup>2</sup>, Shengjun Wang<sup>1</sup>, Fei Kang<sup>1</sup>, Guoquan Li<sup>1</sup>, Orit Jacobson<sup>3</sup>, Gang Niu<sup>3</sup>, Weidong Yang<sup>1</sup>, Jing Wang<sup>1</sup>✉, Xiaoyuan Chen<sup>3</sup>✉

1. Department of Nuclear Medicine, Xijing Hospital, Fourth Military Medical University, Xi'an, China
2. Department of Neurosurgery, Tangdu Hospital, Fourth Military Medical University, Xi'an, China
3. Laboratory of Molecular Imaging and Nanomedicine, National Institute of Biomedical Imaging and Bioengineering (NIBIB), National Institutes of Health (NIH), Bethesda, Maryland 20892, United States

\* Zhe Wang and Mingru Zhang contributed equally to this article.

✉ Corresponding authors: Jing Wang, E-mail: wangjing@fmmu.edu.cn or Xiaoyuan Chen, E-mail: shawn.chen@nih.gov

© 2015 Ivyspring International Publisher. Reproduction is permitted for personal, noncommercial use, provided that the article is in whole, unmodified, and properly cited. See <http://ivyspring.com/terms> for terms and conditions.

Received: 2015.04.01; Accepted: 2015.04.20; Published: 2015.04.28

## Abstract

**Purpose:** The chemokine receptor CXCR4 is overexpressed in various types of human cancers. As a specific imaging agent of CXCR4,  $^{68}\text{Ga}$ -NOTA-NFB was investigated in this study to assess its safety, biodistribution and dosimetry properties in healthy volunteers, and to preliminarily evaluate its application in glioma patients.

**Methods:** Six healthy volunteers underwent whole-body PET scans at 0, 0.5, 1, 2 and 3 h after  $^{68}\text{Ga}$ -NOTA-NFB injection (mean dose,  $182.4 \pm 3.7$  MBq ( $4.93 \pm 0.10$  mCi)). For time-activity curve calculations, 1 mL blood samples were obtained at 1, 3, 5, 10, 30, 60, 90, 120, 150 and 180 min after the injection. The estimated radiation doses were calculated by OLINDA/EXM software. Eight patients with glioma were enrolled and underwent both  $^{68}\text{Ga}$ -NOTA-NFB and  $^{18}\text{F}$ -FDG PET/CT scans before surgery. The expression of CXCR4 on the resected brain tumor tissues was determined by immunohistochemical staining.

**Results:**  $^{68}\text{Ga}$ -NOTA-NFB was safe and well tolerated by all subjects. A rapid activity clearance from the blood circulation was observed. The organs with the highest absorbed doses were spleen ( $193.8 \pm 32.5$   $\mu\text{Sv}/\text{MBq}$ ) and liver ( $119.3 \pm 25.0$   $\mu\text{Sv}/\text{MBq}$ ). The mean effective dose was  $25.4 \pm 6.1$   $\mu\text{Sv}/\text{MBq}$ . The maximum standardized uptake values ( $\text{SUV}_{\text{max}}$ ) and the maximum target to non-target ratios ( $\text{T}/\text{NT}_{\text{max}}$ ) of  $^{68}\text{Ga}$ -NOTA-NFB PET/CT in glioma tissues were  $4.11 \pm 2.90$  (range, 0.45-8.21) and  $9.21 \pm 8.75$  (range, 3.66-24.88), respectively, while those of  $^{18}\text{F}$ -FDG PET/CT were  $7.34 \pm 2.90$  (range, 3.50-12.27) and  $0.86 \pm 0.41$  (range, 0.35-1.59). The histopathological staining confirmed that CXCR4 was overexpressed on resected tumor tissues with prominent  $^{68}\text{Ga}$ -NOTA-NFB uptake.

**Conclusion:** With a favorable radiation dosimetry profile,  $^{68}\text{Ga}$ -NOTA-NFB is safe for clinical imaging. Compared to  $^{18}\text{F}$ -FDG PET/CT,  $^{68}\text{Ga}$ -NOTA-NFB PET/CT is more sensitive in detecting glioma and could have potential in diagnosing and treatment planning for CXCR4 positive patients.

Key words:  $^{68}\text{Ga}$ -NOTA-NFB, internal dosimetry, CXCR4, glioma, PET/CT

## INTRODUCTION

CXCR4 is a G-protein coupled chemokine receptor with seven transmembrane domains [1]. By binding its ligand CXCL12, the major physiological role of CXCR4 is to mediate chemotaxis of hemato-

poietic cells during homeostasis [2]. CXCR4/CXCL12 axis is also involved in the development of the hematopoietic, cardiovascular, and nervous systems during embryogenesis [3, 4]. Relative to normal tissues,

CXCR4 is over-expressed in many different types of human cancers, including breast, ovarian, melanoma, prostate, lung, and lymphoma [5]. Recent studies have suggested that high expression of CXCR4 in cancers led to tumor metastasis, aggressiveness, poor prognosis, and resistance to chemotherapy [6]. Consequently, the anti-cancer effect of CXCR4/CXCL12 inhibitors has been extensively investigated in clinical trials [5]. To facilitate drug development and patient screening, it is critical to apply non-invasive imaging to evaluate CXCR4 expression in cancer cells.

Several CXCR4 inhibitors or antagonists have been labeled either with  $^{18}\text{F}$ ,  $^{68}\text{Ga}$  or  $^{64}\text{Cu}$  for PET imaging including AMD3100, Pentixafor, and T140 [7-11]. T140, a 14-residue peptide possessing disulfide bond, was initially identified as an anti-HIV agent due to its strong binding with CXCR4 [12]. NOTA-NFB was modified from T140 with improved pharmacokinetics, which consists of 14 amino acids, one disulfide bridge between Cys<sup>4</sup> and Cys<sup>13</sup>, and a macrocyclic NOTA chelator for radionuclide labeling [13]. In the preclinical imaging studies, NOTA-NFB displayed highly specific accumulation in CXCR4-positive tumors and high tumor-to-background ratios, suggesting the feasibility of NOTA-NFB for clinical translation for cancer detection.

Gliomas are the most common malignant brain tumors, characterized by extensive, diffuse infiltrative growth into the surrounding brain parenchyma and different degrees of neovascularization [14-16]. According to WHO, gliomas are classified to four grades, with grades I-II being low-grade glioma (LGG), and grades III-IV being high-grade glioma (HGG) [17]. However, the diagnostic accuracy of the most commonly used  $^{18}\text{F}$ -FDG is confounded by high physiologic glucose metabolism in the brain area, which significantly limits the sensitivity for glioma detection and the specificity for border demarcation [18]. Therefore, more specific radiotracers for PET to assess glioma are highly desirable. Previous studies found that CXCR4 was overexpressed in glioma, especially in malignant glioma [19, 20]. A CXCR4 antagonist labeled with  $^{11}\text{C}$  was tested in a C6 rat glioma model with modest tumor/muscle contrast [21].

In this study, for the first time, we labeled NOTA-NFB with  $^{68}\text{Ga}$  and applied this tracer for CXCR4 evaluation in glioma patients after measuring the dosimetry of  $^{68}\text{Ga}$ -NOTA-NFB in healthy volunteers.

## MATERIALS AND METHODS

### $^{68}\text{Ga}$ -NOTA-NFB Preparation

NOTA-NFB was synthesized according to a published procedure [13] using NOTA-NHS ester

(CheMatech) as a chelator.  $^{68}\text{Ga}$ -NOTA-NFB (Figure 1) was synthesized by the following protocol: 50  $\mu\text{g}$  of NOTA-NFB (5  $\mu\text{g}/\mu\text{L}$  in deionized water) was added into a mixture of 50  $\mu\text{L}$  of sodium acetate solution (1.25 M) and 1 mL of  $^{68}\text{GaCl}_3$  eluent (370–666 MBq, pH 1.3–1.5) obtained from a  $^{68}\text{Ge}/^{68}\text{Ga}$  generator (ITG Co., Germany). The mixture was then heated at 100 °C for 10 min. The reaction mixture was quenched by adding 10 mL of water and was then loaded onto a pre-activated C-18 Sep-pak Plus cartridge (500 mg, Waters). The cartridge was washed with an additional 6 mL of water. The radiolabeled peptide was eluted with 1 mL of 10 mM HCl/ethanol. The resulting solution was analyzed by instant thin-layer chromatography (ITLC, Bioscan, USA) and HPLC (Agilent Technologies 1200, USA). ITLC was performed with silica-gel paper strips (VARIAN) in a 1:1 mixture of methanol and sodium acetate developing solution. Analytical HPLC was performed on an Agilent Technologies 1200 system equipped with a RP C-18 column (ZORBAX, 5  $\mu\text{m}$ , 4.6  $\times$  250 mm). The HPLC method: solvent A consisted of 0.05% trifluoroacetic acid (TFA) in water, and Solvent B consisted of 0.05% TFA in acetonitrile with a flow rate of 1 mL/min. Gradient: 0–3 min, 5–5% solvent B; 3–20 min, 5–65% solvent B. The final  $^{68}\text{Ga}$ -NOTA-NFB solution was filtered with a 0.22  $\mu\text{m}$  Millex-GP filter (EMD Millipore) before the injection.

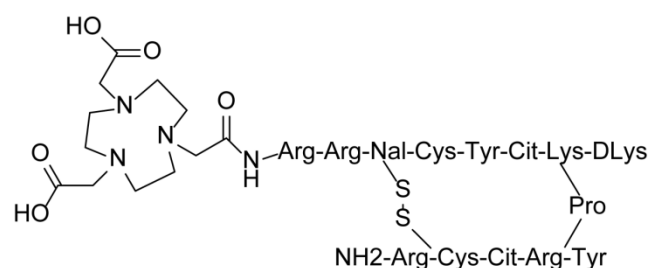


Fig. 1. Structure of NOTA-NFB.

### Subjects

This study (ClinicalTrials.gov identifier: NCT02327442) was approved by the Independent Ethics Committee of Xijing Hospital and written informed consent was obtained from all the subjects. Six healthy volunteers (3 F, 3 M; mean age 48  $\pm$  11 y; age range, 37–61 y) were recruited based on their medical history, physical examination, electrocardiogram, urinalysis, and standard blood tests. Eight newly diagnosed glioma patients (6 F, 2 M; mean age 52  $\pm$  13 y; age range, 30–73 y; 2 LGG and 6 HGG were confirmed by pathological analysis after surgery) were included based on their clinical symptoms and magnetic resonance imaging (MRI). The exclusion criteria were

pregnancy, lactation, hepatic and renal insufficiency and inability to complete the needed examinations. The demographic characteristics of the healthy volunteers and glioma patients were listed in Tables 1 and 2, respectively.

**Table 1.** Demographic characteristics of the enrolled healthy volunteers

No.	Gender	Age (years)	Weight (Kg)	Height (cm)	Injected Activity (mCi)
1	F	40	51	160	4.91
2	M	39	64	170	4.98
3	F	37	48	154	4.76
4	M	61	62	158	4.88
5	M	60	67	173	5.04
6	F	49	49	154	4.99
Mean ± SD		48 ± 11	57 ± 8	162 ± 8	4.93 ± 0.10

**Table 2.** Demographic characteristics of the enrolled glioma patients

No.	Gender	Age (years)	Weight (Kg)	WHO grading	Disease Duration	Pathology	Location
1	F	44	57	II	1 M	oligoastrocytoma	frontal lobe
2	F	30	49	II	3 D	oligoastrocytoma	frontal, temporal lobe
3	M	61	84	III	2 M	oligoastrocytoma	frontal lobe
4	F	60	65	IV	3 M	glioblastoma	occipital lobe
5	F	73	57	IV	2 M	glioblastoma	temporal lobe
6	F	53	67	IV	6 M	glioblastoma	frontal
7	M	43	79	IV	20 D	glioblastoma	frontal
8	F	54	73	IV	15 M	glioblastoma	occipital lobe

### Biodistribution and Dosimetry in Healthy Volunteers

$^{68}\text{Ga}$ -NOTA-NFB in the range of 4.76-5.04 mCi (176.12-186.48 MBq) was injected to the healthy subjects within 30 seconds. The PET scans were acquired at 0, 30, 60, 120 and 180 min after tracer injection using a Biograph 40 system (Siemens Medical Solutions, Erlangen, Germany), with seven bed positions (2 min/bed, from head to the proximal thighs). Low-dose CT scans for attenuation correction were acquired (automatic mAs, 120 keV, 512 × 512 matrix, 5 mm slice thickness, 1.0 s rotation time, and 0.8 pitch). PET scans were acquired for 2 min/bed. The imaging field ranged from head to the proximal thighs. The PET/CT images were transferred to a multimodal workstation (Syngo TrueX and HD Truepoint Siemens Medical Solutions) for data analysis. Regions of interest (ROIs) were outlined over the major organs based on the contour of CT images. For the bone

marrow dose calculation, we used the image-based method and chose the lumbar vertebrae L2-L4 to outline the ROI.

$\text{SUV}_{\text{max}}$  of the major organs were obtained from the corresponding PET images, then according to the function, organ activities at different time points were calculated. Time-activity curves were integrated using the GraphPad Prism software (version 5, GraphPad Software, Inc., USA). The individual normalized number of disintegrations were used for calculating effective doses for the standard 70-kg adult male model with OLINDA/EXM (Version 1.1, Vanderbilt University, 2007) for each patient separately [22, 23].

1 mL blood samples were obtained at 1, 3, 5, 10, 30, 60, 90, 120, 150 and 180 min after tracer injection. After centrifugation, the radioactivity in red blood cells and plasma was measured with a Gamma counter. Vital signs (heart rate, pulse oximetry value, body temperature, and blood pressure) were monitored every 15 min to ensure the safety of the subjects.

### PET/CT Scans of Glioma Patients

All eight patients underwent both  $^{68}\text{Ga}$ -NOTA-NFB and  $^{18}\text{F}$ -FDG PET/CT scans. For each patient, 1.48-2.96 MBq (0.04-0.08 mCi) per kilogram of  $^{68}\text{Ga}$ -NOTA-NFB was injected intravenously. Head CT scans for attenuation correction were acquired (200 mAs, 120 keV, 512 × 512 matrix, 3 mm slice thickness, 1.0 s/rotation, and 0.8 pitch), followed by brain PET acquisition at 40 min post-injection of  $^{68}\text{Ga}$ -NOTA-NFB (1 bed position, 10 min duration).  $^{18}\text{F}$ -FDG PET/CT was acquired for each patient within 3 days of  $^{68}\text{Ga}$ -NOTA-NFB scan. Patients fasted for at least 4 h before the  $^{18}\text{F}$ -FDG was injected at a dosage of 0.15 mCi per kilogram of body weight. PET/CT images were independently reviewed by 3 experienced nuclear medicine physicians.

### Immunohistochemical Staining

Resected tissues from all eight patients were sliced, followed by immunohistochemical staining to evaluate the expression of CXCR4. Briefly, 5- $\mu\text{m}$ -thick tissue sections from all primary tumors were stained for the CXCR4 protein using a primary rabbit polyclonal antibody (Abcam, clone 2074; Cambridge, UK). Slides were deparaffinized through a series of xylene baths. Then rehydration was performed through graded alcohols. The sections were then immersed in methanol containing 0.3% hydrogen peroxide for 20 min to block endogenous peroxidase activity and incubated in 2.5% blocking serum to reduce nonspecific binding. Sections were subsequently incubated overnight at 4 °C with primary anti-CXCR4 antibody at dilutions of 1:1000. Detection of the primary antibody was performed by incubation with peroxi-

dase-conjugated affinitive goat anti-rabbit IgG (ZB-2301, ZSGB-BIO, Beijing). As a chromogen, 3,3'-diaminobenzidine (DAB) was used. Sections were rinsed, counterstained with hematoxylin (Sigma-Aldrich Inc.) [21]. After washing, coverslips were mounted and sections were examined under an Olympus DP72 microscope.

### Statistical Analysis

The difference test of  $SUV_{max}$  and  $T/NT_{max}$  between  $^{68}Ga$ -NOTA-NFB PET/CT and  $^{18}F$ -FDG PET/CT was through paired *t*-test. All the statistical analyses were performed by GraphPad Prism software (version 5, GraphPad Software, Inc., USA), and  $p < 0.05$  was considered statistically significant.

## RESULTS

### Radiochemistry

The decay-corrected radio chemical yield (RCY) of  $^{68}Ga$ -NOTA-NFB was  $74 \pm 3\%$  ( $n = 5$ ) and the radiochemical purity (RCP) tested by HPLC was nearly 100%.

### Biosafety

The weights of six healthy volunteers were  $57 \pm 8$  kg (range, 48-67 kg) and the average injection dose of

$^{68}Ga$ -NOTA-NFB was  $4.93 \pm 0.10$  mCi (range, 4.76-5.04 mCi) (Table 1), with the mean specific radioactivity level of 7.4-9.9 MBq/nmol. As such, the mean mass of tracer injected to each subject was 21-64 nmol or 16.7-50  $\mu$ g. The administration of  $^{68}Ga$ -NOTA-NFB was safe and well tolerated. No significant changes in vital signs, electrocardiograms, or clinical laboratory blood tests were observed during the imaging period.

### Biodistribution and Dosimetry in Healthy Volunteers

The radioactivity was accumulated predominantly in the spleen and urinary bladder at 1 h after injection, followed by liver, kidneys and the red marrow (Fig. 2A). The activity in the spleen decreased quickly over time. The initial uptakes in the liver and kidneys were moderate, which increased over time, while that in the kidneys remained virtually unchanged (Fig. 2B). There was a rapid clearance of the activity from the blood circulation (Fig. 2C). Based on the time-activity curves for  $^{68}Ga$ -NOTA-NFB in the blood samples, majority of the tracer was found in the plasma with negligible accumulation in the red blood cells.

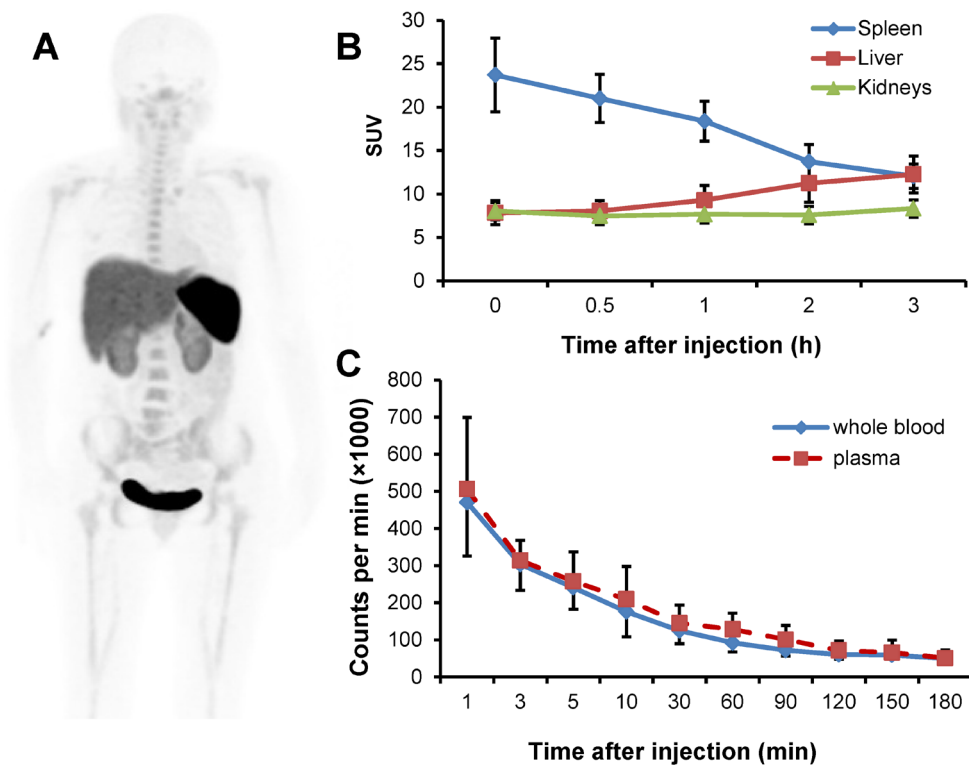


**Fig. 2.** **A.** PET image of distribution of  $^{68}Ga$ -NOTA-NFB 1 h after injection in a healthy volunteer (subject 3). The uptake is mainly in the spleen, liver, kidneys and urinary bladder. **B.** Decay corrected averaged time-activity curves of  $^{68}Ga$ -NOTA-NFB in the liver, kidneys and spleen for all healthy volunteers. Error bars indicate standard deviations ( $n = 6$ ). **C.** Decay corrected averaged time-activity curves for  $^{68}Ga$ -NOTA-NFB in the whole blood and plasma determined by gamma counter. Error bars indicate standard deviations ( $n = 6$ ).

The mean normalized number of disintegrations in units of hours of the source organs and remainder of the body are listed in Table 3. The largest mean normalized number of disintegrations for the subjects was found in the remainder tissues ( $0.47 \pm 0.12$  MBq-h/MBq), followed by muscle ( $0.37 \pm 0.04$  MBq-h/MBq) and liver ( $0.34 \pm 0.34$  MBq-h/MBq).

**Table 3.** Normalized number of disintegrations of source organs for subjects injected with  $^{68}\text{Ga}$ -NOTA-NFB

Target	Mean	SD
	MBq-h/MBq	MBq-h/MBq
Adrenals	0.0016	0.0003
Brain	0.0038	0.0002
Breasts	0.0047	0.0012
Gallbladder Contents	0.0007	0.0001
LLI	0.0062	0.0005
Small Intestine	0.0206	0.0009
Stomach	0.0068	0.0021
ULI	0.0062	0.0006
Heart Contents	0.0000	0.0000
Heart Wall	0.0139	0.0031
Kidneys	0.0487	0.0002
Liver	0.3712	0.0375
Lungs	0.0123	0.0013
Muscle	0.3390	0.0226
Ovaries	0.0003	0.0001
Pancreas	0.0054	0.0001
Red Marrow	0.0751	0.0352
Cortical Bone	0.0000	0.0000
Trabecular Bone	0.0000	0.0000
Spleen	0.0677	0.0024
Thymus	0.0006	0.0000
Thyroid	0.0015	0.0001
Urinary Bladder Contents	0.0150	0.0122
Uterus/Uterine Wall	0.0038	0.0013
Remainder	0.4692	0.1153

The absorbed doses of various tissues were shown in Table 4. The organ with the highest absorbed dose was spleen ( $193.8 \pm 32.5$   $\mu\text{Sv}/\text{MBq}$ ), followed by liver ( $119.3 \pm 25.0$   $\mu\text{Sv}/\text{MBq}$ ), kidneys ( $84.9 \pm 9.4$   $\mu\text{Sv}/\text{MBq}$ ) and adrenals ( $55.2 \pm 15.7$   $\mu\text{Sv}/\text{MBq}$ ). On the other hand, brain absorbed very low dose ( $2.7 \pm 0.6$   $\mu\text{Sv}/\text{MBq}$ ), suggesting that  $^{68}\text{Ga}$ -NOTA-NFB does not readily cross intact blood-brain barrier (BBB). The mean effective dose was  $25.4 \pm 6.1$   $\mu\text{Sv}/\text{MBq}$ .

### $^{68}\text{Ga}$ -NOTA-NFB and $^{18}\text{F}$ -FDG PET/CT Scans for Glioma

There was barely any uptake of  $^{68}\text{Ga}$ -NOTA-NFB in normal brain tissues, including the white matter and the cortical gray matter, with the rather low  $\text{SUV}_{\text{max}}$  of  $0.11 \pm 0.02$  (range, 0.10-0.13). In contrast,  $^{18}\text{F}$ -FDG metabolizes actively in normal brain tissues, resulting in a high background with  $\text{SUV}_{\text{max}}$  of  $9.63 \pm 2.97$  (range, 6.22-15.33). In the glioma patients, specific accumulation of  $^{68}\text{Ga}$ -NOTA-NFB was observed with the  $\text{SUV}_{\text{max}}$  of  $4.11 \pm 2.90$  (range, 0.45-8.21) (Table 5), which was significantly different from that of  $^{18}\text{F}$ -FDG

( $p < 0.05$ ), with the  $\text{SUV}_{\text{max}}$  of  $7.34 \pm 2.90$  (range, 3.50-12.27). As a result, the  $\text{T}/\text{NT}_{\text{max}}$  of  $^{68}\text{Ga}$ -NOTA-NFB ( $9.21 \pm 8.75$ , range: 3.7-24.9) was significantly higher than that of  $^{18}\text{F}$ -FDG ( $0.86 \pm 0.41$ , range: 0.35-1.59) ( $p < 0.05$ ), indicating that  $^{68}\text{Ga}$ -NOTA-NFB is superior to  $^{18}\text{F}$ -FDG in determining the boundary of glioma. Furthermore, we found that the  $\text{SUV}_{\text{max}}$  and  $\text{T}/\text{NT}_{\text{max}}$  of  $^{68}\text{Ga}$ -NOTA-NFB in HGG were much higher than those in LGG, with the  $\text{SUV}_{\text{max}}$  and  $\text{T}/\text{NT}_{\text{max}}$  for 6 HGG being  $5.32 \pm 2.19$  (range, 2.55-8.21) and  $11.34 \pm 9.26$  (range, 3.66-24.88), respectively, while for 2 the LGG patients, the  $\text{SUV}_{\text{max}}$  were 0.45 and 0.54, and the  $\text{T}/\text{NT}_{\text{max}}$  were 2.7 and 3.0.

**Table 4.** Radiation dosimetry of  $^{68}\text{Ga}$ -NOTA-NFB

Target	Mean	SD
	$\mu\text{Sv}/\text{MBq}$	$\mu\text{Sv}/\text{MBq}$
Adrenals	55.2	15.7
Brain	2.7	0.6
Breasts	8.9	1.6
Gallbladder Wall	17.9	3.5
Lower large intestine wall	17.6	3.0
Small Intestine	20.2	3.1
Stomach Wall	16.3	4.8
Upper large intestine wall	15.9	3.2
Heart Wall	28.7	0.9
Kidneys	84.9	9.4
Liver	119.3	25.0
Lungs	11.3	2.2
Muscle	11.0	3.7
Ovaries	18.3	3.1
Pancreas	36.8	3.5
Red Marrow	19.1	7.5
Osteogenic Cells	19.6	8.7
Skin	5.7	1.6
Spleen	193.8	32.5
Thymus	16.5	2.4
Thyroid	35.0	14.8
Urinary Bladder Wall	28.9	12.5
Uterus	27.2	6.9
Total Body	17.3	9.3
Effective Dose Equivalent	39.2	7.6
Effective Dose	25.4	6.1

**Table 5.** Comparison of  $\text{SUV}_{\text{max}}$  and  $\text{T}/\text{NT}_{\text{max}}$  between  $^{68}\text{Ga}$ -NOTA-NFB and  $^{18}\text{F}$ -FDG

No.	WHO grading	$^{68}\text{Ga}$ -NOTA-NFB		$^{18}\text{F}$ -FDG	
		$\text{SUV}_{\text{max}}$	$\text{T}/\text{NT}_{\text{max}}$	$\text{SUV}_{\text{max}}$	$\text{T}/\text{NT}_{\text{max}}$
1	II	0.45	3.00	7.40	0.72
2	II	0.54	2.70	3.50	0.35
3	III	8.21	24.88	7.27	0.61
4	IV	6.60	21.29	12.27	0.80
5	IV	6.83	4.71	5.76	0.72
6	IV	2.55	6.07	9.87	0.78
7	IV	4.01	7.43	8.47	1.36
8	IV	3.73	3.66	4.20	1.59
<i>p</i>		0.03*	0.03 <sup>†</sup>		

\*The *p* value of  $\text{SUV}_{\text{max}}$  between  $^{68}\text{Ga}$ -NOTA-NFB and  $^{18}\text{F}$ -FDG.

<sup>†</sup>The *p* value of  $\text{T}/\text{NT}_{\text{max}}$  between  $^{68}\text{Ga}$ -NOTA-NFB and  $^{18}\text{F}$ -FDG.

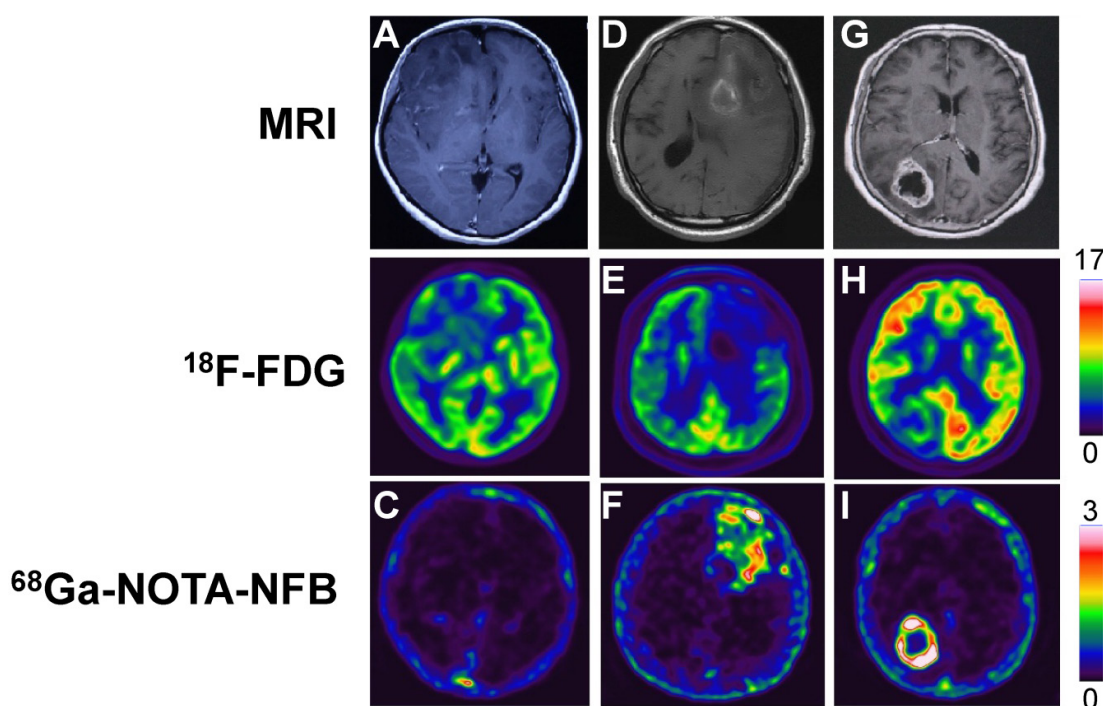


**Fig. 3.** Comparison of MRI,  $^{18}\text{F}$ -FDG PET and  $^{68}\text{Ga}$ -NOTA-NFB PET in three different glioma patients. In the upper row, **A & G** are enhanced MRI by administration of gadolinium contrast agent and **D** is MRI without contrast enhancement. The middle row shows  $^{18}\text{F}$ -FDG PET and the lower row shows  $^{68}\text{Ga}$ -NOTA-NFB PET. The first column (**A, B & C**): Patient No. 2, F, 30 y, grade II; the second column (**D, E & F**): Patient No. 3, M, 61 y, grade III; the third column (**G, H & I**): Patient No. 4, F, 60 y, grade IV.

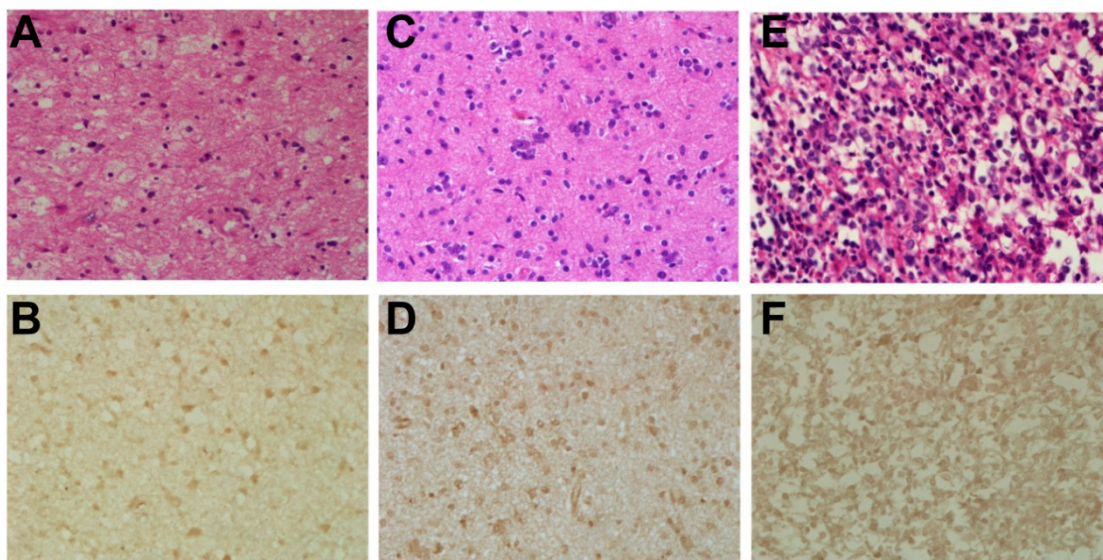


**Fig. 4.** Hematoxylin-eosin (H&E) and immunohistochemical stains of glioma samples. Upper row (**A, C & E**): hematoxylin-eosin stains, magnification 400 $\times$ ; lower row (**B, D & F**): immunohistochemical stains of CXCR4, magnification 400 $\times$ . The first column (**A & B**): F, 30 y, grade II; the second column (**C & D**): M, 61 y, grade III; the third column (**E & F**): F, 60 y, grade IV.

### Histopathological Features and Immunohistochemical Staining of Tumor Tissue

Hematoxylin-eosin (H&E) and the immunohistochemical staining for CXCR4 were performed in glioma tissues from all 8 patients. Two tumors were graded as WHO II, 1 tumor as WHO III and 5 tumors as WHO IV respectively, according to the H&E staining. For all 8 tumors, the expression of CXCR4 in the

resected glioma tissues was confirmed to be positive. The expression of CXCR4 varies from different pathological grades, with low expression for grade II, and high for grade III-IV (Fig. 4), which corroborates with the  $\text{SUV}_{\text{max}}$  of  $^{68}\text{Ga}$ -NOTA-NFB PET.

### DISCUSSION

CXCR4 is overexpressed in more than 23 human cancers [24]. It is involved in three fundamental as-

pects of cancers: primary tumor growth, cancer cell migration, and establishment of metastatic sites; and therefore, it can be considered as an ideal target for imaging [25]. Many peptidic and small molecular ligands with different modes of antagonistic activity have been developed so far, among which, NOTA-NFB is a specific inhibitor of CXCR4 receptor and has been previously labeled with  $^{64}\text{Cu}$  for imaging tumor CXCR4 expression [13]. In this investigation, we first assessed the biodistribution and dosimetric properties of  $^{68}\text{Ga}$ -NOTA-NFB and then evaluated its potential for glioma diagnosis.

$^{68}\text{Ga}$ -NOTA-NFB had prominent uptake in the liver and spleen. The high uptake in the spleen can be explained by its high physiological expression of CXCR4, and also this result is in line with the imaging study of CXCR4 in mice [7, 8]. However, CXCR4 expression in the liver is limited to hematopoietic cells and stellate cells. The high uptake of this tracer in the liver may be due to the presence of metal chelators, which may undergo transchelation under physiological condition. High accumulation of  $^{68}\text{Ga}$ -NOTA-NFB was also detected in the kidneys and the urinary bladder, possibly due to the hydrophilicity and relatively small size of the peptide. The rapid blood clearance may commonly be due to the fast renal excretion of peptide tracers.

The effective dose of  $^{68}\text{Ga}$ -NOTA-NFB reported here (25.4  $\mu\text{Sv}/\text{MBq}$ ) is comparable to those of  $^{68}\text{Ga}$ -DOTA-TOC (23  $\mu\text{Sv}/\text{MBq}$ ),  $^{68}\text{Ga}$ -DOTA-NOC (25  $\mu\text{Sv}/\text{MBq}$ ), and  $^{68}\text{Ga}$ -NOTA-RGD (22  $\mu\text{Sv}/\text{MBq}$ ) [23]. With an injected dose of 5 mCi (185 MBq), the subject would be exposed to an effective radiation dose of 4.70 mSv. This dose is a little bit higher than another recently reported CXCR4 targeting agent,  $^{68}\text{Ga}$ -pentixafor [11, 26, 27]. However, it is much lower than the dose limit of 0.5 Sv per year, as set forth by the Food and Drug Administration [22]. According to the calculated dosimetric values (spleen demonstrated the highest absorbed dose, 193.8  $\mu\text{Sv}/\text{MBq}$ ), a maximum of 70 mCi (2.58 GBq) of  $^{68}\text{Ga}$ -NOTA-NFB per patient can be injected per year, or up to 14 acquisitions can be performed in one patient per year by 5 mCi (185 MBq) per scan. This supports the use of  $^{68}\text{Ga}$ -NOTA-NFB in repeated PET scans, for example, in therapeutic monitoring.

$^{18}\text{F}$ -FDG, the most commonly used PET tracer in the nuclear medicine clinic, has been extensively investigated in the diagnosis of various human cancers and cardiovascular diseases. However, the application in brain tumors is limited due to the high normal brain background, resulting from the vigorous glucose metabolism of the brain. Thus, an effective imaging agent with high accumulation in the tumor and low background in the normal brain is desirable.

Glioma is the most common primary brain tumor and accounts for nearly half of all brain tumors [14]. Recently, numerous studies have reported that chemokine receptor CXCR4 was overexpressed in glioma and could be a target for glioma diagnosis. To the best of our knowledge, this is the first PET imaging study conducted in humans to visualize CXCR4 expression for preoperative, noninvasive measurement of glioma.  $^{68}\text{Ga}$ -NOTA-NFB specifically accumulated in glioma and was vacant in normal brain tissues. On the contrary,  $^{18}\text{F}$ -FDG showed less accumulation in glioma than the normal brain tissues. Compared to  $^{18}\text{F}$ -FDG PET/CT, the favorable  $\text{SUV}_{\text{max}}$  and high  $\text{T}/\text{NT}_{\text{max}}$  of  $^{68}\text{Ga}$ -NOTA-NFB PET/CT could improve the sensitivity of glioma diagnosis. Lately,  $^{68}\text{Ga}$ -NOTA-PRGD2 was applied to detect glioma by targeting integrin  $\alpha_v\beta_3$  [17].  $^{68}\text{Ga}$ -NOTA-PRGD2 was found to have high accumulation in the glioma, and low uptakes in the normal brain except for the choroid plexus. Compared to the significant accumulation of  $^{68}\text{Ga}$ -NOTA-PRGD2 in choroid plexus,  $^{68}\text{Ga}$ -NOTA-NFB was absent in that area, which enable it to diagnose cerebroventricular neoplasms.

The information obtained from the histopathological staining confirmed that CXCR4 was overexpressed on glioma, and was consistent with the  $\text{SUV}_{\text{max}}$  of  $^{68}\text{Ga}$ -NOTA-NFB, indicating that CXCR4 could be a target in evaluating glioma. We also noticed that the CXCR4 expression and  $\text{SUV}_{\text{max}}$  of  $^{68}\text{Ga}$ -NOTA-NFB in HGG was much higher than that of LGG, suggesting that  $^{68}\text{Ga}$ -NOTA-NFB may be capable of evaluating glioma grades. However, due to the limited number of recruited patients, especially LGG, we are unable to correlate the CXCR4 expression with glioma grades in this study. Further investigations with larger number and various grades of glioma patients are necessary to evaluate the full potential of  $^{68}\text{Ga}$ -NOTA-NFB in glioma diagnosis and prognosis.

## CONCLUSION

With a favorable radiation dosimetry profile,  $^{68}\text{Ga}$ -NOTA-NFB is safe for clinical imaging. The specific accumulation of  $^{68}\text{Ga}$ -NOTA-NFB in glioma and the clean background in normal brain tissue suggest that  $^{68}\text{Ga}$ -NOTA-NFB may be a valuable tracer in diagnosing and evaluating glioma patients.

## ACKNOWLEDGEMENT

This work was supported by the Key Program of National Natural Science Foundation of China (Grant No. 81230033), the Major State Basic Research Development Program (Grant No. 2011CB707704), the Major Instrument of National Natural Science Foundation Research Project (Grant No. 81227901), the Na-

tional Natural Science Foundation of China (Grant No. 81371594, 81401442, 81371596), the International Cooperation Program of Xijing Hospital (Grant No. XJZT13G02), a Key Science and Technology Program of Shaanxi Province, China (Grant No. 2013K12-03-05). The authors are grateful to Zhiyong Quan, Zhiping Yang, Jin Zeng, Mingxuan Zhao, and Ming Zhang at the Department of Nuclear Medicine, Xijing Hospital, for performing the PET/CT scans and collecting data. We also thank Yi Li from the Department of Neurosurgery, Tangdu Hospital, for immunohistochemical analysis, and Jing Li, from the Department of Pathology, Xijing Hospital, for pathological analysis.

## COMPETING INTERESTS

The authors have declared that no competing interest exists.

## REFERENCES

- Murdoch C. CXCR4: chemokine receptor extraordinaire. *Immunol Rev.* 2000; 177: 175-84.
- Nagasawa T, Hirota S, Tachibana K, Takakura N, Nishikawa S, Kitamura Y, et al. Defects of B-cell lymphopoiesis and bone-marrow myelopoiesis in mice lacking the CXC chemokine PBSF/SDF-1. *Nature.* 1996; 382: 635-8.
- Weiss ID, Jacobson O. Molecular imaging of chemokine receptor CXCR4. *Theranostics.* 2013; 3: 76-84.
- Li M, Ransohoff RM. Multiple roles of chemokine CXCL12 in the central nervous system: a migration from immunology to neurobiology. *Prog Neurobiol.* 2008; 84: 116-31.
- Domanska UM, Kruizinga RC, Nagengast WB, Timmer-Bosscha H, Huls G, de Vries EG, et al. A review on CXCR4/CXCL12 axis in oncology: no place to hide. *Eur J Cancer.* 2013; 49: 219-30.
- Gagliardi F, Narayanan A, Reni M, Franzin A, Mazza E, Boari N, et al. The role of CXCR4 in highly malignant human gliomas biology: current knowledge and future directions. *Glia.* 2014; 62: 1015-23.
- Jacobson O, Weiss ID, Kiesewetter DO, Farber JM, Chen X. PET of tumor CXCR4 expression with 4-<sup>18</sup>F-T140. *J Nucl Med.* 2010; 51: 1796-804.
- Gourni E, Demmer O, Schottelius M, D'Alessandria C, Schulz S, Dijkgraaf J, et al. PET of CXCR4 expression by a <sup>68</sup>Ga-labeled highly specific targeted contrast agent. *J Nucl Med.* 2011; 52: 1803-10.
- Aghanejad A, Jalilian AR, Fazaeli Y, Alirezapoor B, Pouladi M, Beiki D, et al. Synthesis and Evaluation of [<sup>68</sup>Ga]-AMD3100: A Novel Imaging Agent for Targeting the Chemokine Receptor CXCR4. *Sci Pharm.* 2014; 82: 29-42.
- Jacobson O, Weiss ID, Szajek LP, Niu G, Ma Y, Kiesewetter DO, et al. PET imaging of CXCR4 using copper-64 labeled peptide antagonist. *Theranostics.* 2011; 1: 251-62.
- Wester HJ, Keller U, Schottelius M, Beer A, Philipp-Abbrederis K, Hoffmann F, et al. Disclosing the CXCR4 expression in lymphoproliferative diseases by targeted molecular imaging. *Theranostics.* 2015; 5: 618-30.
- Tamamura H, Omagari A, Hiramatsu K, Gotoh K, Kanamoto T, Xu Y, et al. Development of specific CXCR4 inhibitors possessing high selectivity indexes as well as complete stability in serum based on an anti-HIV peptide T140. *Bioorg Med Chem Lett.* 2001; 11: 1897-902.
- Jacobson O, Weiss ID, Szajek LP, Niu G, Ma Y, Kiesewetter DO, et al. Improvement of CXCR4 tracer specificity for PET imaging. *J Control Release.* 2012; 157: 216-23.
- Uemae Y, Ishikawa E, Osuka S, Matsuda M, Sakamoto N, Takano S, et al. CXCL12 secreted from glioma stem cells regulates their proliferation. *J Neurooncol.* 2014; 117: 43-51.
- Liu C, Pham K, Luo D, Reynolds BA, Hothi P, Foltz G, et al. Expression and Functional Heterogeneity of Chemokine Receptors CXCR4 and CXCR7 in Primary Patient-Derived Glioblastoma Cells. *PLoS One.* 2013; 8: 1-12.
- Wang S, Zhang S, Li J, Xu X, Weng Y, Zheng M, et al. CXCL12-induced up-regulation of FOXM1 expression promotes human glioblastoma cell invasion. *Biochem Biophys Res Commun.* 2014; 447: 1-6.
- Li D, Zhao X, Zhang L, Li F, Ji N, Gao Z, et al. <sup>68</sup>Ga-PRGD2 PET/CT in the evaluation of glioma: A prospective study. *Mol Pharm.* 2014; 11: 3923-9.
- la Fougere C, Suchorska B, Bartenstein P, Kreth FW, Tonn JC. Molecular imaging of gliomas with PET: opportunities and limitations. *Neuro Oncol.* 2011; 13: 806-19.
- Gagliardi F, Narayanan A, Reni M, Franzin A, Mazza E, Boari N, et al. The role of CXCR4 in highly malignant human gliomas biology: Current knowledge and future directions. *Glia.* 2014; 62: 1015-23.
- lv S, Sun B, Zhong X, Dai C, Wang W, Ma X, et al. The Clinical Implications of Chemokine Receptor CXCR4 in Grade and Prognosis of Glioma Patients: A Meta-Analysis. *Mol Neurobiol.* 2014 Sep 12. [Epub ahead of print] doi:10.1007/s12035-014-8894-3.
- Hartimath SV, Waarde Av, Dierckx RAJO, Vries EFJd. Evaluation of N-[<sup>11</sup>C]methyl-AMD3465 as a PET tracer for imaging of CXCR4 receptor expression in a C6 glioma tumor model. *Mol Pharm.* 2014; 11: 3810-7.
- Mittra ES, Goris ML, Jagaru AH, Kardan A, Burton L, Berganos R, et al. Pilot pharmacokinetic and dosimetric studies of <sup>18</sup>F-FPPRGD2: a PET radiopharmaceutical agent for imaging  $\alpha v\beta 3$  integrin levels. *Radiology.* 2011; 260: 182-91.
- Roivainen A, Kahkonen E, Luoto P, Borkowski S, Hofmann B, Jambor J, et al. Plasma pharmacokinetics, whole-body distribution, metabolism, and radiation dosimetry of <sup>68</sup>Ga bombesin antagonist BAY 86-7548 in healthy men. *J Nucl Med.* 2013; 54: 867-72.
- Woodard LE, Nimmagadda S. CXCR4-based imaging agents. *J Nucl Med.* 2011; 52: 1665-9.
- Demmer O, Gourni E, Schumacher U, Kessler H, Wester H-J. PET Imaging of CXCR4 Receptors in Cancer by a New Optimized Ligand. *ChemMedChem.* 2011; 6: 1789-91.
- Philipp-Abbrederis K, Herrmann K, Knop S, Schottelius M, Eiber M, Lückereath K, et al. In vivo molecular imaging of chemokine receptor CXCR4 expression in patients with advanced multiple myeloma. *EMBO Mol Med.* 2015. doi:10.15252/emmm.201404698.
- Herrmann K, Lapa C, Wester H-J, Schottelius M, Schiepers C, Eberlein U, et al. Biodistribution and Radiation Dosimetry for the Chemokine Receptor CXCR4-Targeting Probe <sup>68</sup>Ga-Pentixafor. *J Nucl Med.* 2015; 56: 410-6.